# Retro-inversal of Intracellular Selected Aβ Interacting Peptides: Implications for a Novel Alzheimer's Disease Treatment.



| | |
|---|---|
| Journal: | *Biochemistry* |
| Manuscript ID: | bi-2014-001257.R1 |
| Manuscript Type: | Article |
| Date Submitted by the Author: | n/a |
| Complete List of Authors: | Acerra, Nicola; University Of Essex, Biological Sciences<br>Kad, Neil; University Of Essex, Biological Sciences<br>Griffith, Douglas; University of Cambridge, Department of Genetic<br>Ott, Stanislav; University of Cambridge, Department of Genetic<br>Crowther, Damian; University of Cambridge, Department of Genetic<br>Mason, Jody; University Of Essex, Biological Sciences |
| | |

# Retro-inversal of Intracellular Selected Aβ Interacting Peptides: Implications for a Novel Alzheimer's Disease Treatment.

Nicola Acerra[1], Neil. M. Kad[1], Douglas A. Griffith[2], Stanislav Ott[2], Damian C. Crowther[2] and Jody M. Mason[1]

[1]*Department of Biological Sciences, University of Essex, Wivenhoe Park, Colchester, CO4 3SQ, UK Tel +44 1206 873010; Fax +44 1206 872592*

[2]*Department of Genetics, University of Cambridge, Downing Site, Cambridge, CB2 3EH*

[1]*To whom correspondence should be addressed: jmason@essex.ac.uk*

Running title: Retro-inversed intracellular selected A$\beta$ binders

Abbreviations: A$\beta_{1\text{-}42}$, $\beta$-amyloid 1-42 variant; CD, circular dichroism; PPI, Protein-protein Interaction; PCA, Protein-fragment Complementation Assay; MTT, (3-(4,5-Dimethylthiazol-2-yl)-2,5-diphenyltetrazolium bromide; ThT, Thioflavin-T; HFIP, hexafluoroisopropanol; TFA, trifluoroacetic acid; CPP, cell-penetrating peptide; TAT, trans-activating transcriptional activator

Funding: JMM thanks Alzheimer's Research UK for a pilot project grant (ART/PPG2008B/2) and AgeUK for a New Investigator Award (340). JMM is the recipient of a Cancer Research UK Career Establishment Award (A11738) and a Wellcome Trust Project Grant (WT090184MA). NA is funded by a University of Essex Departmental Studentship. JMM and NMK also thank Parkinson's UK for awarding a PhD Studentship (H-1001). DCC is supported by Wellcome Trust (082604/2/07/Z), Medical Research Council UK (G0700990) and an Alzheimer's Research UK Senior Research Fellow (ART-SRF2010-2).

**ABSTRACT:**

The aggregation of $\beta$-amyloid (A$\beta$) into toxic oligomers is a hallmark of Alzheimer's disease pathology. Here we present a novel approach for the development of peptides capable of preventing amyloid aggregation based upon the previous selection of natural all-L peptides that bind A$\beta_{1\text{-}42}$. Using an intracellular selection system, successful library members were further screened via competition selection to identify the most effective peptides capable of reducing amyloid levels. In order to circumvent potential issues arising from stability and protease action for these structures we have replaced all L-residues with D-residues and inverted the sequence. These retro-inverso (RI) peptide analogues therefore encompass reversed sequences that maintain the overall topological order of the native peptides. Our results demonstrate that efficacy in blocking and reversing amyloid formation is maintained while introducing desirable properties to the peptides. Thioflavin-T assays, circular dichroism, and oblique angle fluorescence microscopy collectively indicate that RI-peptides can reduce amyloid load while MTT assays demonstrate modest reductions in cell toxicity. These conclusions are reinforced using *Drosophila melanogaster* studies to monitor pupal hatching rates and fly locomotor activity in the presence of RI-peptides delivered via RI-TAT peptide fusions. We demonstrate that the RI-PCA approach can be used as a generalised method for deriving A$\beta$-interacting peptides. This approach has subsequently led to several peptide candidates to be further explored as potential treatments for Alzheimer's disease.

## INTRODUCTION

A vast body of evidence implicates A$\beta$ as a major player in Alzheimer's Disease (AD) (*1*), with genetic studies revealing abnormal production in cell culture and animal models. A$\beta$ aggregation is implicated in neuronal death and impaired memory (*2*), with a wealth of evidence suggesting that amyloid load in AD sufferers does not correlate with disease severity (*2, 3*). The insoluble fibrils that are characteristic of the disease may serve as reservoirs that sequester a number of more toxic and soluble oligomeric species. Consequently, targeting A$\beta$ via therapeutic intervention has led to numerous inhibition strategies. Rare familial mutations that increase A$\beta$ oligomer concentration (e.g. the E22G arctic mutation (*4*)) have been shown to accelerate the onset of AD as a result (*4*). Many $\beta$-sheet breaker (BSB) molecules that block or breakdown amyloid fibres have had limited success and in certain cases have been counteractive, owing either to increased oligomer production or a failure to accelerate their removal (*5-11*). Therefore, since oligomers as small as dimers have been shown to exhibit cytotoxicity (*12, 13*) molecules effective at lowering amyloid levels may need to either sequester fibrils in the insoluble state, or preferably bind A$\beta$ as a small but ultimately non-toxic oligomer, possibly even the monomer (*14*).

We have previously used intracellular library screening and selection to identify A$\beta$ interacting peptides (*15*). In this approach, residues 25-35 of A$\beta$ are used as a design scaffold. This sequence, along with residues 15-20, is known to form amyloid in isolation (*5, 6*) and is thought to be responsible for instigating A$\beta$ self-association in the parental protein. Many amyloid inhibitors have therefore been based upon these regions (*5-11*) (see also (*16*) and references therein), with many strategies focused on simple modifications such that they retain the ability to bind A$\beta$ but prevent amyloid formation by introducing blocking or charged groups to these short sequences. For example, Tjernberg *et al* demonstrated that $A\beta_{16-20}$, despite forming fibrils itself, binds residues 25–35 of A$\beta$ and prevents fibril formation (*5*).

Soto and co-workers rationally designed proline-containing peptides based on A$\beta_{17-21}$ (*10, 11*). It was subsequently shown that clearance of large amyloid fibrils can lead to the population of smaller more cytotoxic intermediates (*17*). Therefore, the search for BSB peptides has been hampered by the fact that successful molecules must be capable of preventing the population of amyloid oligomers while avoiding the generation of cytotoxic species. In our current approach we use an intracellular protein-fragment complementation assay (PCA) selection, which works by recombining a split enzyme that is essential for cell survival (*15, 18-20*). We apply a variation on this system whereby the A$\beta$ target is fused at the genetic level to one half of the essential enzyme murine dihydrofolate reductase (mDHFR), with a peptide library fused to the other half. Following protein expression in the cytoplasm, binding of a library member to A$\beta$ reconstitutes mDHFR, leading to bacterial cell growth and colony formation under selective conditions. Since the entire process is intracellular, no assumptions are made regarding the mechanism of antagonist action or which amyloid states become populated during selection. The only prerequisite for success of any given library member is therefore that it must *i)* bind to A$\beta$ and reconstitute mDHFR and *ii)* prevent A$\beta$ aggregation that has been shown to slow cell growth, with *E.coli* rescued from the toxic effects of aggregation. In addition, the PCA approach is predicted to select peptides that are resistant to degradation by bacterial proteases, be soluble in solution, and target-specific in the presence of other cytoplasmic proteins. Using PCA with an 8000 member library based on A$\beta_{29-35}$ led to an initial interacting sequence. A second library of 160,000 members using this first hit as a design scaffold yielded two further novel interacting sequences. These peptides consequently shared no homology to the original A$\beta_{29-35}$ design template. All selected peptides were found to be capable of binding A$\beta$, inhibiting amyloid formation and breaking down preformed fibrils.

A potential limitation of this previous study was the use of natural unmodified L-peptides which are susceptible to degradation by mammalian proteases. This was partially

addressed by undertaking library selection inside the cytoplasm of *E.coli*. However, while bacterial growth experiments indicated that toxicity was lowered, cytotoxicity experiments using mammalian cells suggested that protease protection was not observed when transferring to the PC12 cell environment (*15*). In a continuation of the above study we present data on retro-inversed (RI) analogues of these previously selected peptides whereby we have substituted the L-amino acids for their D counterparts and reversed the sequence. The D-amino acid sequences give a mirror conformation, while the retro-peptides, consisting of the same sequence of L-amino acids, leads to a reversal in order. Sequence retro-inversal therefore leads to a mimic of the original peptide owing to inversion of the peptide bonds (*21, 22*). Using this approach peptides have been shown to retain the same inhibitory aggregation qualities while displaying vastly increased protease resistance (*23*). For example, rationally designed RI peptide inhibitors of A*β* aggregation have previously been derived by appending arginine residues to the $A\beta_{16\text{-}20}$ (KLVFF) sequence (*24, 25*). These peptides were also shown to be serum stable and with the addition of a RI cell penetrating peptide fusion were also able to cross the blood brain barrier and display significant activity in transgenic mouse models (*26*). In addition, although not an RI approach, mirror image phage display has been used to screen a 12-mer library against an immobilised D-enantiomer of the $A\beta_{1\text{-}42}$ peptide, with the most successful peptide binder replaced by D-amino acids to yield a protease-stable peptide capable of binding to the natural L-form of $A\beta_{1\text{-}42}$ (*27*). The success of these studies further highlights the potential for peptide-based therapeutic strategies.

Here we report upon a novel approach that uses *intracellular* library screening and selection followed by sequence retro-inversal (RI-PCA) as a generalised strategy for creating stable peptides capable of antagonising protein-protein interactions (PPI). We have tested the effectiveness of peptides using a range of *in vitro* techniques that report on the amount of fibril present. These experiments have been coupled with PC12 neuronal cell-based assays that

report on the overall effect of toxicity in the presence of various peptides, as well as *in vivo* studies using *drosophila melanogaster,* to verify peptide efficacy in the context of a whole cell Alzheimer's disease model organism.

## MATERIALS AND METHODS

***PCA and expression vector cloning -*** PCA has been extensively used to derive PPI antagonists of activator protein-1 (*18, 19, 28, 29*). More recently this has been extended to A$\beta$ interacting peptides, where a full description of the methods can be found (*15*). Briefly, mDHFR was split and one half fused to an A$\beta_{25\text{-}35}$ target peptide, and the other half to the library (*15*). Only target binding library members bring two halves of mDHFR into close proximity, render it active, and lead to colony formation on M9 selective plates. Trimethoprim is used to selectively inhibit bacterial DHFR, thereby ensuring that colonies can only arise as the result of an interaction between A$\beta$ and a peptide-library member. The A$\beta_{25\text{-}35}$ gene was synthesized using overlap extension PCR and cloned into the pES300d-DHFR2 vector system using NheI and AscI restriction sites.

***PCA Library construction*** - Library construction and cloning has been described previously (*15, 18*). Briefly, in the first library, positions 31-33 of A$\beta_{29\text{-}35}$ were completely randomized using degenerate oligonucleotides containing NNK codons. NNK was used to encode all twenty residues while removing two of three stop codons (*30*) to create an 8000 member library. The second library was designed using the first PCA winner ('KAT') as a design scaffold. In this case residues 29-30 and 34-35 of KAT were randomized, again using the codon NNK, this time to generate a library of 160,000 members. Thus in starting with A$\beta_{29\text{-}35}$ as an initial design scaffold a completely unrelated sequence was subsequently derived.

Competition selection during PCA means that only the most effective 1–2 sequences are isolated from the 50–100 A$\beta$ binders that are initially identified during single-step selection.

***Aβ Peptide preparation -*** A$\beta_{1\text{-}42}$ was purchased as a pure recombinant peptide from rPeptide (Stratech) and used for all experiments described. Prior to use, the peptide was treated to three rounds of dissolution in hexofluoro-2-propanol (HFIP), sonication, drying, dissolution in trifluoroacetic acid (TFA), followed by sonication and drying, according to the Zagorski protocol (*31*). Peptide was then aliquoted into appropriately sized batches for subsequent assays and dried via lyophilisation before being dissolved in 10mM potassium phosphate buffer (pH 7.4) to generate a final concentration of 50μM. Rounds of TFA/HFIP treatment were used to ensure that amyloid growth always proceeded from the same monomeric state, thus reducing errors in amyloid growth and consequent assay measurements. For the second library winners, two versions of each peptide was synthesised: (i) the parental sequence including selected residues (L2P1a-RI / L2P2a-RI), and (ii) including additional amino acids from restriction sites during cloning into the pES230d vector (L2P1b-RI / L2P2b-RI) (*15*). See Table 1 for all peptide sequences.

***Peptide preparation*** – KAT-RI, L2P1a-RI, L2P1b-RI, L2P2a-RI, L2P2b-RI and both a positive control from the literature, iA$\beta$5 (*10*), and a negative control peptide, TAT-dummy-RI, were obtained by Peptide Protein Research (Fareham, UK) as pure lyophilised peptides. In addition, for *drosophila melanogaster* experiments, TAT-KAT-RI, TAT-L2P1-RI and TAT-L2P2-RI were also used. Peptides were weighed using an analytical balance and stock solutions of 1mM concentration were subsequently dissolved in ultrapure water. Prior to assay peptides were either aliquoted and lyophilised or diluted from stock as required.

***Thioflavin T Assays -*** ThT inhibition assays were performed using 50 μM Zagorski treated (*31*) monomeric A$\beta_{1\text{-}42}$ in 100 μl of 10 mM potassium phosphate buffer, pH 7.4, with or without each peptide at a concentration of 5μM (for 1:0.1 molar ratio), 50μM (for 1:1 molar ratio), 100μM (for 1:2 molar ratio) and 200μM (for 1:4 molar ratio). In addition, for sub-stoichiometric experiments 0.5 μM (1:0.01 molar ratio), 50 nM (1:0.001 molar ratio) and 5 nM (1:0.0001 molar ratio) were also included to demonstrate progressively reduced activity as the peptide dose is increasingly lowered, thus demonstrating a trend of dose dependency. To achieve this, sufficient A$\beta_{1\text{-}42}$ was lyophilized, dissolved, and thoroughly vortexed as one single batch (for immediate use in all A$\beta_{1\text{-}42}$ target-peptide mixes) to a concentration of 50μM in potassium phosphate buffer. Each inhibitor was lyophilized and redissolved in an Eppendorf tube to a concentration of 5 μM (1:0.1), 50 μM (1:1), 100 μM (1:2), and 200μM (1:4). Finally, a 100 μL aliquot of the target solution was added to each inhibitor to give a total assay volume of 100 μL containing 50 μM target and the appropriate inhibitor. The assay mixture was vortexed and stored at 37°C for three days to induce aggregation in the presence of each inhibitor. The ThT assay solution was prepared from a 25x stock containing 500μM ThT. The stock was aliquoted and kept frozen until required. It was then allowed to thaw at room temperature for 10min before dilution into 10mM Tris buffer pH 7.4, giving the required freshly prepared ThT assay solution containing 20μM ThT in 10mM Tris and buffer at pH 7.4. A total of 197.1 μL of the ThT assay solution was then added into 2.9 μL of each inhibition/reversal assay mixture, thoroughly vortexed and transferred into an appropriate well of the multiplate. The fluorescence of amyloid-bound ThT was measured by florescence spectroscopy using a Cary Eclipse fluorescence spectrophotometer; bound ThT exhibits a new excitation maxima at 450nm and an enhanced emission maxima at 482nm (*32*). For the inhibition assays, the A$\beta_{1\text{-}42}$ target-peptide mixtures were incubated together on day zero at 37°C and single ThT readings were taken on day three. For the reversal assays, the target was

incubated alone at 37°C for three days before the addition of 100 μL to each lyophilized inhibitor. The vortexed A$\beta_{1\text{-}42}$ target-peptide solutions were then incubated at 37°C for a further three days, at which single ThT readings were taken.

***Circular Dichroism (CD) -*** Far-UV circular dichroism (CD) spectra were recorded on an Applied Photophysics Chirascan CD spectrometer at 20°C. Peptide (10μM in 10mM Potassium Phosphate buffer pH 7.4) was added to a 1mm CD cell (Hellma) and spectra recorded over the 200-300 nm range at a scan rate of 10nm/min with step size of 1nm. Spectra were recorded as the average of two scans as raw ellipticity. Spectra for RI-peptides alone were subtracted from A$\beta_{1\text{-}42}$ target + peptide spectra, to leave normalised CD spectra accounting for the effect of the peptide upon the A$\beta_{1\text{-}42}$.

***3-(4,5.Dimethylthiazol-2-yl)-2,5-diphenyltetrazolium Bromide (MTT) Cell-Toxicity Assay -*** MTT experiments were undertaken using Rat phaeochromocytoma (PC12) cells to assess the effect of the toxicity of A$\beta_{1\text{-}42}$. PC12 cells are known to be particularly sensitive and their use in this assay is well established (*33*). The MTT Vybrant® MTT Cell Proliferation Assay Kit (Invitrogen) was used to measure the conversion of the water soluble MTT dye to formazan, which is then solubilized, and the concentration determined by a colour change monitored via absorbance measurement at 570 nm. The change in absorbance can then be converted to a percentage MTT reduction which can be used as an indicator of the PC12 cell health in the assay. The assay was performed with 10 μM A$\beta_{1\text{-}42}$ and varying molar ratios of peptide corresponding to 1:0.1 (0.1 μM), 1:1 (10 μM), 1:2 (20 μM), 1:4 (40 μM). PC12 cells were maintained in RPMI 1640 +2mM glutamine medium mixed with 10% horse serum, 5% foetal bovine serum, supplemented with a 20mg/mL gentamycin. Cells were transferred to a sterile 96-well plate with 30,000 cells per well and experiments performed in triplicate. Briefly,

different concentrations of peptides were screened in the presence of 10 μM A$\beta_{1\text{-}42}$. The required volume from peptide and target stock solutions was freeze-dried overnight. The freeze-dried peptide and A$\beta_{1\text{-}42}$ target were resuspended in 100% dimethyl sulfoxide (DMSO), each at 100x stock concentration (i.e. 1 mM, 2 mM, 4 mM or 10 mM). For example for the molar ratio 1:1 a total of 5 μL from each of the resuspended peptide/DMSO and target/DMSO was mixed in a well of a 96-well preparation plate, thus giving 10μl of 1:1 mM peptide/A$\beta_{1\text{-}42}$ target concentration ratio in 100% DMSO. A total of 90 μL of RPMI media was added to the 10 μL peptide/A$\beta_{1\text{-}42}$ target mixture (100:100 μM peptide/A$\beta_{1\text{-}42}$ target ratio in 10% DMSO). A total of 10 μL of the 50:50 μM peptide/A$\beta_{1\text{-}42}$ target mixture in 10% DMSO was then dispensed into 90 μL of media/PC12 cells, at final peptide peptide and A$\beta_{1\text{-}42}$ target concentrations of 10 μM. These were incubated for 24 h at 37 °C, 5% $CO_2$, prior to the addition of the MTT dye. A total of 10 μL of the day was added to each well and incubated for a further 4h at 37 °C, 5% $CO_2$. A total of 100 μL of the DMSO (stop/solubilisation solution) was then added to each well and was allowed to stand for 10 minutes. The absorbance was measured at 570 nm using a 96-well Versamax tuneable microplate reader.

***Oblique Angle Fluorescence Microscopy Experiments -*** Samples were imaged on a custom built oblique angle fluorescence system as described previously (OAF, (*15, 34*)). The excitation and emission wavelengths were 488 nm and 500-605 nm respectively. Although both the excitation and emission wavelengths were off peak for ThT, the image quality and photobleaching characteristics were excellent. All samples were pre-stained with 10 μM ThT, pipetted onto a clean glass slide, air dried and then imaged in KPP buffer supplemented with 100 mM DTT to further minimize photobleaching. For consistency and cross-correlation, the same samples were used for inhibition/reversal imaging as those in ThT and CD experiments. In addition, all samples provided for OAF imaging were supplied blind.

***Drosophila Melanogaster Assays*** **–** The effect of RI peptides upon *drosophila melanogaster* was assayed by fusing sequences to the (also retro-inversed) nine residue cell-penetrating peptide (CPP), TAT (*35-37*). In these experiments, flies expressing A$\beta_{1\text{-}42}$ were fed nutrient containing either RI-peptides or RI-TAT-peptide fusions (see Table 1) and two key effects monitored; ***i)*** the speed of pupae hatching in which the cumulative hatching fractions for each treatment was monitored relative to a negative control group ***ii)*** fly motility using an automated fly tracking system to monitor the walking speed of the transgenic flies. In the control group, flies typically become immobile as they age over the first 10-15 days of life.

**RESULTS**

We have previously undertaken PCA screening on libraries to derive peptides capable of clearing A$\beta_{1\text{-}42}$ aggregates and generating significant enhancements in bacterial growth rates (*15*). To produce peptides that retain the ability to bind A$\beta_{1\text{-}42}$ while bringing additional properties to the molecule such as stability and protease resistance (*23, 38*) we have now retro-inversed these sequences. The RI-PCA derived peptides (Table 1) have been synthesized and characterised using a number of methods including ThT dye fluorescence to report on amyloid formation, CD to measure global changes in $\beta$-sheet content associated with fibril formation, and direct imaging using OAF microscopy. These techniques have demonstrated that RI-peptides retain the ability of the PCA selected parental peptides to prevent aggregation and remove preformed fibrils. In addition, MTT cytotoxicity assays undertaken using a neuronal PC12 cell line were used to demonstrate that A$\beta_{1\text{-}42}$ toxicity is lowered when bacterially selected peptides (which were not effective in MTT experiments (*15*)) are retro-inversed in sequence. To explore cell-based experiments further, we have undertaken studies in which

*drosophila melanogaster* expressing wild-type A$\beta_{1\text{-}42}$ were fed RI-peptides as well as RI-TAT-peptide fusions to bring cell permeability to these A$\beta_{1\text{-}42}$ interacting compounds.

***ThT binding indicates reduced fibril load -*** To determine the ability of PCA derived peptides to either prevent fibril assembly (inhibition) and/or breakdown preformed fibrils (reversal), ThT was used as an indicator of the degree to which A$\beta_{1\text{-}42}$ had aggregated into amyloid fibrils. In this assay A$\beta_{1\text{-}42}$ was rendered monomeric (*31*) and redissolved at a concentration of 50 μM before being aggregated by incubating without agitation at 37°C. For the inhibition assay, peptides were added on day zero, whereas for the reversal assay the peptides were added after three days of A$\beta_{1\text{-}42}$ fibril growth. Once incubated together, A$\beta_{1\text{-}42}$ target-peptide solutions were tested after three days. In addition to the five RI-PCA derived peptides, the positive control L-peptide iA$\beta$5 was also included as it is known to perform well in ThT assays and lead to a reduction in fibril load (*11*). Finally a negative control peptide TAT-dummy-RI was included to demonstrate no effect on ThT binding and therefore specificity for the PCA-derived peptides. Figure 1 shows the results of these experiments at a number of A$\beta_{1\text{-}42}$:peptide ratios for each peptide. Experiments were undertaken at stoichiometries of 1:0.0001, 1:0.001, 1:0.01, 1:0.1, 1:1, 1:2 and 1:4.

Inhibition experiments demonstrate that peptides are able to prevent aggregation (Figure 1a) with reductions in ThT bound relative to the A$\beta_{1\text{-}42}$ control of up to 80%. During these experiments, a concentration dependence was observed as the Aβ:peptide ratio was lowered (Figure 1). At increasingly higher stoichiometries this trend was less apparent. For example, L2P1a-RI lowered bound ThT by ~30-40% at Aβ:peptide stoichiometries of 1:0.01 of greater. Similarly, L2P2b-RI was also able to reduce bound ThT by >40%. RI-peptides incubated in the absence of Aβ did not bind ThT, displayed weakly helical CD spectra, and were soluble to high concentrations in stock solutions. The lack of concentration dependence

for ThT assays at higher molar ratios is likely to be due to signal-to-noise difficulties, as is shown by consistently large errors that are typical of this assay. In addition, ThT is known to exhibit different fluorescence levels according to the oligomeric state populated (*39*). Given that there are a number of potential intermediates in the growth of A*β*, different fluorescence intensities could result. Reassuringly, the all L-residue positive control peptide, iA*β*5 (*11*) performed well, providing a reduction of 60-80%, that was lost in a dose dependent manner at lower Aβ:iAβ5 ratios. In addition the negative control TAT-dummy-RI peptide had no effect over a range of molar ratios, again demonstrating specificity for the PCA-derived sequences. RI peptides performed favourably relative to their PCA-derived L-peptide counterparts.

In the case of reversal experiments (Figure 1b), as was observed previously for the L-peptide counterparts, more pronounced reductions are observed relative to inhibition experiments; over 60% for all peptides tested in all but six instances. At molar ratios of 1:0.1 reductions of >60% were observed for all peptides. Increasing the molar ratio did not lead to improvements in reversal of amyloid in most cases, indicating that a ten-fold sub-stoichiometric concentration of peptide may be sufficient to reverse fibril formation. As we previously reported for parental L-peptides, a progressively reduced activity was observed as the peptide dose tended towards zero, demonstrating a dose dependency (*15*). Experiments on RI-peptides in isolation indicate that peptides do not aggregate into fibrils. They do not bind ThT and do not generate CD spectra consistent with a β-sheet structure. Again, as predicted from the literature, iA*β*5 performed well at higher molar ratios, and this effect is lost at lower ratios. These results compare favourably with PCA-derived L-peptide counterparts in being able to reduce the ThT bound by ~60% (*15*). Again, the negative control TAT-dummy-RI peptide also had no effect over a range of molar ratios. Errors associated with ThT experiments preclude more detailed interpretations from being drawn.

***CD studies indicate reduced β-sheet content*** – Owing to the fact that amyloid fibrils are predominantly $\beta$-sheet, we have used CD as a measure of the global signal upon incubation with peptides in inhibition and reversal assays. In these experiments the same aggregating samples as used in ThT experiments have been measured to allow for direct comparison between experiments. However, CD experiments in which the aggregating all L-residue A$\beta_{1\text{-}42}$ target is mixed with D-residue containing RI-peptides must be approached with caution; in incubating the peptides together with A$\beta_{1\text{-}42}$ it was unknown if a signal at 218 nm caused by the RI-peptides might obscure the signal at 218 nm arising from the A$\beta_{1\text{-}42}$ target. Therefore, the CD signal of A$\beta_{1\text{-}42}$ and RI-peptides were both measured in isolation. The CD spectra arising from these controls could then be accounted for (i.e. CD spectra of A$\beta_{1\text{-}42}$ *against* [A$\beta_{1\text{-}42}$ + RI-peptide] – [RI-peptide alone]; Figure 2), allowing the overall loss or gain in β-sheet signal exerted by the action of RI-peptide upon A$\beta$ aggregation to be established. In this assay we observe impressive reductions in $\beta$-sheet content for all peptides at various molar ratios, supporting the ThT data by demonstrating that RI-peptides reduce the global $\beta$-sheet content of the sample and therefore the amyloid content. In agreement with the ThT data the negative control peptide TAT-dummy-RI had little effect on the CD signal demonstrating Aβ specificity for the PCA-derived sequences.

***ThT and CD experiments demonstrate that RI peptides do not aggregate in isolation*** - ThT experiments and Circular Dichroism spectroscopy experiments undertaken on RI-peptides in isolation that have been incubated at 50 μM for three days under conditions identical to aggregation assays using Aβ$_{1\text{-}42}$ demonstrate that peptides do not bind significant amounts of ThT, and that the CD signal for all peptides (at 0:1) is consistent with that of a random coil or weakly helical conformation. They therefore indicate along with computational aggregation

prediction programs on the L-residue parent peptides (e.g. Waltz (*40*), Amylpred (*41*), Pasta (*42*), Zyggregator (*43*), and Tango (*44*) that peptides do not form amyloid in isolation.

***MTT experiments indicate reduced amyloid toxicity to cells -*** MTT ((3-(4,5-Dimethylthiazol-2-yl)-2,5-diphenyltetrazolium bromide)) cell toxicity experiments were performed using Rat phaeochromocytoma (PC12) neuronal-like cells to assess toxicity of A$\beta_{1\text{-}42}$ and the preventative effects of the peptides generated in this study. MTT assays (Fig. 4) were preformed across A$\beta_{1\text{-}42}$ target:RI-peptide ratios and normalised relative to cells in isolation (normalised as 0% death) and cells incubated with A$\beta_{1\text{-}42}$ alone (normalised as 100% death). Peptides did not improve cell viability when incubated at 1:0.1. At the increased ratio of 1:1 a decrease in toxicity of between ~30 % was observed for all RI-peptides studied. At increased molar ratios of 1:2 and 1:4 a decrease in toxicity of approximately 10-20% was observed for all RI-peptides studied. This experiment demonstrates a modest but significant reduction in A$\beta_{1\text{-}42}$ induced toxicity in the presence of RI-peptides. This was more promising than for the PCA derived L-peptide parent molecules (*15*) and more impressive than the *iAβ5* peptide which has been previously shown to perform poorly in MTT cytotoxicity experiments using the PC12 cell-line (*7*). Reassuringly, the TAT-dummy-RI peptide had minimal effect of the viability of PC12 cells incubated with Aβ.

***Oblique Angle Fluorescence (OAF) Microscopy indicates a reduction in amyloid levels –*** To allow direct comparison, samples used in ThT and CD experiments were also imaged using OAF microscopy (*34*) for both inhibition and reversal experiments. To prevent bias toward any one sample the experiment was carried out blind. This technique allows for surface associated and stacked aggregates of amyloid fibres to be imaged directly. OAF also permits assessment of the amount of protein deposited as amyloid and its morphology. To further quantify the

amount of amyloid deposited we analysed the mean fluorescence value for each condition using ImageJ (NIH, USA) over a randomly chosen 160x160 pixel$^2$ area and found a similar correlation. In studying the peptides' effects on reversal we found KAT-RI, L2P1b-RI and L2P2a-RI were the most potent, resulting in the fewest observed fibrils on the surface. Also consistent with the reduction in ThT bound, L2P1a-RI and L2P1b-RI appear to have removed the vast majority of fibrils present in the solution. Finally L2P2b-RI displays a number of deposits that are smaller and of different morphology to the A$\beta_{1\text{-}42}$ sample.

OAF microscopy data for inhibition experiments demonstrated that fibrils are present in iA$\beta$5, L2P1a-RI, L2P1b-RI, L2P2a-RI and L2P2b-RI samples. However the average intensity of these fibrils was reduced relative to A$\beta_{1\text{-}42}$. KAT-RI stood out as the one sample with reduced fluorescence intensity and no appearance of fibrils on the surface indicating that KAT-RI reduced the deposition of amyloid. Collectively these data suggest that KAT-RI is most effective overall, while L2P1b-RI and L2P2a-RI are also effective at reversal.

***Retro-Inverso Peptides Rescue Developmental Delay in a* Drosophila *Model of Aβ Toxicity* -** Our initial experiments used retinal expression of the Arctic (E22G) variant of A$\beta_{1\text{-}42}$ to screen for amelioration of the expected rough eye phenotype. The flies were treated with RI peptides in the food throughout larval development. Upon eclosion the severity of the phenotype was scored by investigators blind to the treatment history. No differences in the rough eye phenotype, as compared to untreated flies, could be detected for any of the peptides (data not shown). We did however notice that some treated flies appeared to hatch either earlier or later than normal. When we formally assessed the hatching times of flies, expressing wild type A$\beta_{1\text{-}42}$, we found that two RI peptides lacking a TAT sequence led to an increase in the hatching time as compared to untreated control flies expressing A$\beta_{1\text{-}42}$ (Fig. 6A, left panel). In addition we saw three significant differences for TAT-containing peptides. Considering the A$\beta_{1\text{-}42}$-

expressing flies we found that those treated with the TAT-L2P2-RI peptide hatched significantly earlier while those treated with TAT-KAT-RI and TAT-L2P1-RI, which were comparable to water-fed controls. Surprisingly treatment with a poly-gly dummy peptide linked to the TAT sequence resulted in a more severe developmental delay as compared to untreated flies (Fig. 6B, right panel). This sequence reassuringly demonstrates that the effect of improved hatching is sequence specific, with this control sequence having the opposite effect. As an additional control, non-transgenic flies were treated with TAT-L2P2-RI and TAT-dummy-RI peptide; these flies hatched at the same time as control flies treated with water (data not shown) suggesting that the effects on development are Aβ-specific.

***Retro-Inverso Peptides Promote Locomotor Activity in a Drosophila Model of Aβ Toxicity-*** The expression of A$\beta$ peptides in the nervous system of the fly is known to reduce the walking velocity of flies with increasing age. To determine whether A$\beta_{1\text{-}42}$–expressing flies treated with RI peptides might retain their locomotor function for longer. As we can see from Fig. 7A, left panel, when we treated flies with RI peptides lacking a TAT sequence, there were only small effects on the walking velocity, particularly for flies younger than 5 days. Those peptides that carry a TAT sequence (Fig 7B, right panel) also increased the walking velocity of young A$\beta_{1\text{-}42}$–expressing flies. In particular flies treated with the TAT-L2P1-RI peptide exhibited markedly increased walking velocities.

***Retro-inversed peptides have minimal effect on the presence of plaques -*** Oral administration of RI peptides did not alter the pattern of A$\beta_{42}$ deposits in the *Drosophila* brain (Figure 8). Flies treated with KAT-RI, L2P1-RI, L2P2-RI, TAT-KAT-RI, TAT-L2P1-RI, TAT-L2P2-RI, TAT-Dummy-RI and water all appeared to exhibit similar deposits of Aβ-reactive material

(arrow, stained with 6E10 antibody), suggesting that although amyloid deposits recognised by this antibody have not been abolished, the production of toxic species has been modulated.

## DISCUSSION

The PPI field has long been considered undruggable using conventional small molecules, while peptide-based approaches have gained considerable traction in recent years (*23, 38*). This owes to the fact that PPIs feature extended interacting surfaces with many points of contact that are too shallow to accommodate traditional small molecule inhibitors, making peptides and their mimetics promising candidates for intervention. Peptides often form highly specific interactions with their target and many associated barriers (e.g. cell permeability and bioavailability) can now be addressed via a number of modification options. To develop peptide inhibitors of Aβ amyloidosis, we have combined a Protein-fragment Complementation Assay (PCA) approach with semi-rational library design, and PCA screening. This has been followed by retro-inversal of the selected peptide sequences to identify molecules capable of binding $A\beta_{1\text{-}42}$ and lowering toxicity. The process has been iterative; the initial library search used the $A\beta_{29\text{-}35}$ sequence as a design scaffold, and the second library design was based on the initial winner, to yield a completely unrelated sequence to the parent template. By retro-inversing these PCA library-selected sequences we aimed to increase peptide bioavailability while retaining desirable inhibitory properties. Our results demonstrate that the inhibitory properties found in the L-peptide templates are retained in the RI sequences. For both inhibition and reversal ThT experiments we observed a reduction in the ThT-bound to $A\beta_{1\text{-}42}$ upon incubation with RI-sequences. Reassuringly the reduction in ThT bound is less at increasingly sub-stoichiometric peptide concentrations, demonstrating a dose dependency. ThT data is supported by a large decrease in the global β-sheet CD signal upon examination of the same samples. These experiments therefore suggest

that RI-peptides can bind A$\beta_{1\text{-}42}$ and exert their effect by reducing the amount of the protein in amyloid form. The reduction in CD signal was more pronounced than for ThT reflecting that the assays measure different outputs. Thus while fibrils are being broken down into smaller structures with significantly less $\beta$-sheet content, the species that become populated are still able to bind ThT, although to a lesser extent than for A$\beta_{1\text{-}42}$ in isolation. In addition, as was observed for L-peptides, the reduction in ThT bound is more pronounced for reversal experiments, suggesting that RI-peptides are more effective at reversing preformed fibrils than preventing amyloid assembly. RI-Peptides in isolation displayed either random coil or weakly helical spectra, perhaps indicating a mechanism of binding that involves a structural change in the target protein. MTT cytotoxicity data additionally indicate that although at sub-stoichiometric ratios RI-peptides are effective at reducing β-sheet content and ThT-binding, they are ineffective at causing a reduction in A$\beta_{1\text{-}42}$ toxicity. For this to be achieved molar ratios of 1:1 or greater are required. This reduction in toxicity is modest (~30% at most), suggesting that although populated amyloid species are not toxic to the bacteria in which they were selected, the reduction in toxicity is however reduced when transferred to the context of a mammalian line. Since bacterial cells harbouring parental L-peptide-DHFR2 fusions have demonstrated an improvement in DHFR activity as well as increased bacterial doubling rates, this suggests that toxicity reduction is successful within the confines of the selection system. One possibility to circumvent this issue and improve outputs from the MTT assay would be to use libraries based on existing sequences while transferring the PCA selection to a therapeutically relevant neuronal cell line (*20*). However, testing these RI compounds in *Drosophila melanogaster* has demonstrated that several sequences can go on to improve either hatching rates or locomotor activity, with TAT-L2P2-RI being the most striking for the former and TAT-L2P1-RI for the latter. Lastly, the presence of comparable brain plaque levels for each of the peptides suggests that amyloid deposits recognised by this antibody

have not been abolished. Interpreting this result alongside fly hatching times and locomotor activity data suggests that the production of the toxic Aβ species has been modulated. These results compare favourably with ThT, CD, OAF microscopy and MTT studies in demonstrating that peptides function by modulating amyloid levels and consequently reducing associated cytotoxicity. The RI-PCA approach therefore offers the potential to derive protease resistant A*β*-interacting peptides that are capable of lowering the toxicity associated with amyloid, which may in turn serve as potential precursors for an Alzheimer's disease treatment.

**ACKNOWLEDGEMENTS**

The authors wish to thank Dr Miao Yu and Dr Victoria Allen-Baume for excellent technical assistance throughout the project.

**REFERENCES**

1. Karran, E., Mercken, M., and De Strooper, B. (2011) The amyloid cascade hypothesis for Alzheimer's disease: an appraisal for the development of therapeutics, *Nat Rev Drug Discov 10*, 698-712.
2. Haass, C., and Selkoe, D. J. (2007) Soluble protein oligomers in neurodegeneration: lessons from the Alzheimer's amyloid beta-peptide, *Nat Rev Mol Cell Biol 8*, 101-112.
3. McLean, C. A., Cherny, R. A., Fraser, F. W., Fuller, S. J., Smith, M. J., Beyreuther, K., Bush, A. I., and Masters, C. L. (1999) Soluble pool of Abeta amyloid as a determinant of severity of neurodegeneration in Alzheimer's disease, *Ann Neurol 46*, 860-866.
4. Nilsberth, C., Westlind-Danielsson, A., Eckman, C. B., Condron, M. M., Axelman, K., Forsell, C., Stenh, C., Luthman, J., Teplow, D. B., Younkin, S. G., Naslund, J., and

Lannfelt, L. (2001) The 'Arctic' APP mutation (E693G) causes Alzheimer's disease by enhanced Abeta protofibril formation, *Nat Neurosci 4*, 887-893.

5. Tjernberg, L. O., Naslund, J., Lindqvist, F., Johansson, J., Karlstrom, A. R., Thyberg, J., Terenius, L., and Nordstedt, C. (1996) Arrest of beta-amyloid fibril formation by a pentapeptide ligand, *J Biol Chem 271*, 8545-8548.

6. Hughes, E., Burke, R. M., and Doig, A. J. (2000) Inhibition of toxicity in the beta-amyloid peptide fragment beta -(25-35) using N-methylated derivatives: a general strategy to prevent amyloid formation, *J Biol Chem 275*, 25109-25115.

7. Kokkoni, N., Stott, K., Amijee, H., Mason, J. M., and Doig, A. J. (2006) N-Methylated peptide inhibitors of beta-amyloid aggregation and toxicity. Optimization of the inhibitor structure, *Biochemistry 45*, 9906-9918.

8. Tjernberg, L. O., Callaway, D. J., Tjernberg, A., Hahne, S., Lilliehook, C., Terenius, L., Thyberg, J., and Nordstedt, C. (1999) A molecular model of Alzheimer amyloid beta-peptide fibril formation, *J Biol Chem 274*, 12619-12625.

9. Gordon, D. J., Sciarretta, K. L., and Meredith, S. C. (2001) Inhibition of beta-amyloid(40) fibrillogenesis and disassembly of beta-amyloid(40) fibrils by short beta-amyloid congeners containing N-methyl amino acids at alternate residues, *Biochemistry 40*, 8237-8245.

10. Soto, C., Kindy, M. S., Baumann, M., and Frangione, B. (1996) Inhibition of Alzheimer's amyloidosis by peptides that prevent beta-sheet conformation, *Biochem Biophys Res Commun 226*, 672-680.

11. Soto, C., Sigurdsson, E. M., Morelli, L., Kumar, R. A., Castano, E. M., and Frangione, B. (1998) Beta-sheet breaker peptides inhibit fibrillogenesis in a rat brain model of amyloidosis: implications for Alzheimer's therapy, *Nat Med 4*, 822-826.

12. O'Nuallain, B., Freir, D. B., Nicoll, A. J., Risse, E., Ferguson, N., Herron, C. E., Collinge, J., and Walsh, D. M. (2010) Amyloid beta-protein dimers rapidly form stable synaptotoxic protofibrils, *J Neurosci 30*, 14411-14419.

13. O'Nuallain, B., Klyubin, I., Mc Donald, J. M., Foster, J. S., Welzel, A., Barry, A., Dykoski, R. K., Cleary, J. P., Gebbink, M. F., Rowan, M. J., and Walsh, D. M. (2011) A monoclonal antibody against synthetic Abeta dimer assemblies neutralizes brain-derived synaptic plasticity-disrupting Abeta, *J Neurochem 119*, 189-201.

14. Giuffrida, M. L., Caraci, F., Pignataro, B., Cataldo, S., De Bona, P., Bruno, V., Molinaro, G., Pappalardo, G., Messina, A., Palmigiano, A., Garozzo, D., Nicoletti, F., Rizzarelli, E., and Copani, A. (2009) Beta-amyloid monomers are neuroprotective, *J Neurosci 29*, 10582-10587.

15. Acerra, N., Kad, N. M., and Mason, J. M. (2013) Combining Intracellular Selection with Protein-fragment Complementation to Derive Aβ interacting Peptides, *Protein Eng Des Sel 26*, 463-470.

16. Doig, A. J. (2007) Peptide inhibitors of beta-amyloid aggregation, *Curr Opin Drug Discov Devel 10*, 533-539.

17. Lowe, T. L., Strzelec, A., Kiessling, L. L., and Murphy, R. M. (2001) Structure-function relationships for inhibitors of beta-amyloid toxicity containing the recognition sequence KLVFF, *Biochemistry 40*, 7882-7889.

18. Pelletier, J. N., Campbell-Valois, F. X., and Michnick, S. W. (1998) Oligomerization domain-directed reassembly of active dihydrofolate reductase from rationally designed fragments, *Proc Natl Acad Sci U S A 95*, 12141-12146.

19. Mason, J. M., Schmitz, M. A., Muller, K. M., and Arndt, K. M. (2006) Semirational design of Jun-Fos coiled coils with increased affinity: Universal implications for leucine zipper prediction and design, *Proc Natl Acad Sci U S A 103*, 8989-8994.

20. Remy, I., Campbell-Valois, F. X., and Michnick, S. W. (2007) Detection of protein-protein interactions using a simple survival protein-fragment complementation assay based on the enzyme dihydrofolate reductase, *Nat Protoc 2*, 2120-2125.

21. Chorev, M., and Goodman, M. (1995) Recent developments in retro peptides and proteins--an ongoing topochemical exploration, *Trends Biotechnol 13*, 438-445.

22. Fletcher, M. D., and Campbell, M. M. (1998) Partially Modified Retro-Inverso Peptides: Development, Synthesis, and Conformational Behavior, *Chem Rev 98*, 763-796.

23. Mason, J. M. (2010) Design and development of peptides and peptide mimetics as antagonists for therapeutic intervention, *Future Med Chem 2*, 1813-1822.

24. Matharu, B., El-Agnaf, O., Razvi, A., and Austen, B. M. (2010) Development of retro-inverso peptides as anti-aggregation drugs for beta-amyloid in Alzheimer's disease, *Peptides 31*, 1866-1872.

25. Taylor, M., Moore, S., Mayes, J., Parkin, E., Beeg, M., Canovi, M., Gobbi, M., Mann, D. M., and Allsop, D. (2010) Development of a proteolytically stable retro-inverso peptide inhibitor of beta-amyloid oligomerization as a potential novel treatment for Alzheimer's disease, *Biochemistry 49*, 3261-3272.

26. Parthsarathy, V., McClean, P. L., Holscher, C., Taylor, M., Tinker, C., Jones, G., Kolosov, O., Salvati, E., Gregori, M., Masserini, M., and Allsop, D. (2013) A novel retro-inverso peptide inhibitor reduces amyloid deposition, oxidation and inflammation and stimulates neurogenesis in the APPswe/PS1DeltaE9 mouse model of Alzheimer's disease, *PLoS One 8*, e54769.

27. Wiesehan, K., Buder, K., Linke, R. P., Patt, S., Stoldt, M., Unger, E., Schmitt, B., Bucci, E., and Willbold, D. (2003) Selection of D-Amino-Acid peptides that bind to

Alzheimer's disease amyloid peptide A beta(1-42) by mirror image phage display, *Chembiochem 4*, 748-753.

28. Mason, J. M., Muller, K. M., and Arndt, K. M. (2007) Positive aspects of negative design: simultaneous selection of specificity and interaction stability, *Biochemistry 46*, 4804-4814.

29. Mason, J. M., Hagemann, U. B., and Arndt, K. M. (2009) Role of hydrophobic and electrostatic interactions in coiled coil stability and specificity, *Biochemistry 48*, 10380-10388.

30. Virnekas, B., Ge, L., Pluckthun, A., Schneider, K. C., Wellnhofer, G., and Moroney, S. E. (1994) Trinucleotide phosphoramidites: ideal reagents for the synthesis of mixed oligonucleotides for random mutagenesis, *Nucleic Acids Res 22*, 5600-5607.

31. Zagorski, M. G., Yang, J., Shao, H., Ma, K., Zeng, H., and Hong, A. (1999) Methodological and chemical factors affecting amyloid beta peptide amyloidogenicity, *Methods Enzymol 309*, 189-204.

32. LeVine, H., 3rd. (1993) Thioflavine T interaction with synthetic Alzheimer's disease beta-amyloid peptides: detection of amyloid aggregation in solution, *Protein Sci 2*, 404-410.

33. Shearman, M. S., Ragan, C. I., and Iversen, L. L. (1994) Inhibition of PC12 cell redox activity is a specific, early indicator of the mechanism of beta-amyloid-mediated cell death, *Proc Natl Acad Sci U S A 91*, 1470-1474.

34. Kad, N. M., Wang, H., Kennedy, G. G., Warshaw, D. M., and Van Houten, B. (2010) Collaborative dynamic DNA scanning by nucleotide excision repair proteins investigated by single- molecule imaging of quantum-dot-labeled proteins, *Mol Cell 37*, 702-713.

35. Frankel, A. D., and Pabo, C. O. (1988) Cellular Uptake of the Tat Protein from Human Immunodeficiency Virus, *Cell 55*, 1189-1193.

36. Fawell, S., Seery, J., Daikh, Y., Moore, C., Chen, L. L., Pepinsky, B., and Barsoum, J. (1994) Tat-Mediated Delivery of Heterologous Proteins into Cells, *P Natl Acad Sci USA 91*, 664-668.

37. Morris, M. C., Deshayes, S., Heitz, F., and Divita, G. (2008) Cell-penetrating peptides: from molecular mechanisms to therapeutics, *Biology of the Cell 100*, 201-217.

38. Craik, D. J., Fairlie, D. P., Liras, S., and Price, D. (2013) The future of peptide-based drugs, *Chem Biol Drug Des 81*, 136-147.

39. Biancalana, M., and Koide, S. (2010) Molecular mechanism of Thioflavin-T binding to amyloid fibrils, *Biochim Biophys Acta 1804*, 1405-1412.

40. Maurer-Stroh, S., Debulpaep, M., Kuemmerer, N., Lopez de la Paz, M., Martins, I. C., Reumers, J., Morris, K. L., Copland, A., Serpell, L., Serrano, L., Schymkowitz, J. W., and Rousseau, F. (2010) Exploring the sequence determinants of amyloid structure using position-specific scoring matrices, *Nat Methods 7*, 237-242.

41. Frousios, K. K., Iconomidou, V. A., Karletidi, C. M., and Hamodrakas, S. J. (2009) Amyloidogenic determinants are usually not buried, *BMC Struct Biol 9*, 44.

42. Trovato, A., Seno, F., and Tosatto, S. C. (2007) The PASTA server for protein aggregation prediction, *Protein Eng Des Sel 20*, 521-523.

43. Tartaglia, G. G., and Vendruscolo, M. (2008) The Zyggregator method for predicting protein aggregation propensities, *Chem Soc Rev 37*, 1395-1401.

44. Fernandez-Escamilla, A. M., Rousseau, F., Schymkowitz, J., and Serrano, L. (2004) Prediction of sequence-dependent and mutational effects on the aggregation of peptides and proteins, *Nat Biotechnol 22*, 1302-1306.

## FIGURE LEGENDS

**Figure 1:** ThT Inhibition and Reversal Data. The data in a) and b) show the effects of different stoichiometries of the peptides KAT-RI, L2P1a-RI, L2P1b-RI, L2P2a-RI, and L2P2b-RI on the aggregation of 50μM A$\beta_{1\text{-}42}$ (at three days for the inhibition assay and at six days for reversal assay). Molar ratios (Aβ:peptide) are shown at 1:0.0001, 1:0.001, 1:0.01, 1:0.1, 1:1, 1:2 and 1:4 for each peptide. iAβ5 and TAT-dummy-RI are included as positive and negative controls respectively. Errors are given as the standard deviation of all errors at each molar ratio. The data show that for the three lowest molar ratios (all sub-stoichiometric; 1:0.01, 1:0.001, and 1:0.0001) the average reduction in ThT bound was minimal (106% for Inhibition and 89% for reversal). In contrast at the three highest molar ratios the reduction in ThT bound was significantly greater (58% for inhibition, 38% for reversal). The most effective average molar ratio for peptides was 1:0.1 which displayed ThT bound values of 35% and 26% for inhibition and reversal, approximating to 71% and 63% less than the average of the three lowest stoichiometries respectively.

**Figure 2:** Circular Dichroism spectra show i) β-sheet content of RI peptides with Aβ ii) RI peptides alone and iii) with RI-peptides subtracted from the combined signal (i.e. ii) – i)). This is shown at all molar molar ratios studied for inhibition and reversal conditions. Both experiments are undertaken at three days postmix and performed at a concentration 10μM A$\beta_{1\text{-}42}$.

**Figure 3:** Circular Dichroism spectroscopy and ThT experiments undertaken on RI-peptides in isolation that have been incubated at 50 μM for three days under conditions identical to aggregation assays using A$\beta_{1\text{-}42}$.

**Figure 4:** MTT toxicity assay using A$\beta_{1\text{-}42}$ and selected RI-peptides using different molar ratios after 24 hours of incubation. The assay was performed with 10 μM A$\beta_{1\text{-}42}$ and different concentrations of inhibitor, for example, 1:0.1 (1 μM ), 1:1 (10 μM), 1:2 (20 μM), 1:4 (40 μM).

**Figure 5:** Oblique Angle Fluorescence (OAF) Microscopy data. During reversal experiments, A$\beta_{1-42}$ was grown alone for three days, after which RI-peptide was added at a stoichiometry of 1:4 and followed by a further three day incubation to assay for peptide induced reversal of amyloid deposition. Each sample was then imaged by fluorescence microscopy and panels showing representative images obtained. To quantify amyloid deposition the mean grey value over a 160x160 pixel area randomly chosen for five separate images is plotted as fluorescence intensity. Each data point is normalized to the control iAβ5 peptide by subtraction. Shown are a) Inhibition data and b) Reversal data. It can be clearly seen that both KAT and L2P1B are strongly inhibitory for this reversal assay. The scale bars represent a distance of 2 μm. Each data point was then scaled to overcome the 'background noise' by taking Aβ (1:0) as the maximum.

**Figure 6:** Oral administration of RI peptides suppresses the delayed eclosion associated with pan-neuronal expression of A$\beta_{42}$. A) As compared to A$\beta_{42}$ treated with water (control), those flies treated with KAT-RI and L2P1-RI showed small but significant suppression of the developmental delay ($p<0.05$). B) Upon fusion with the TAT peptide the potency of the RI peptides increased with TAT-KAT-RI ($p<0.05$) and TAT-L2P2-RI ($p<0.001$) exhibiting significant suppression of delayed eclosion as compared to water (control). Oral administration of a dummy RI peptide resulted in significant increase in the delay in eclosion ($p<0.05$). Significance determined by the log-rank test.

**Figure 7**: Oral administration of RI peptides suppresses the locomotor deficits associated with pan-neuronal expression of A$\beta_{42}$. A) As compared to flies treated with water (control), flies

receiving RI peptides recorded higher walking velocities in the first days of adult life. The rank order of velocities was L2P1>L2P2>KAT>control. B) Upon fusion with the TAT peptide the potency of the TAT-L2P1-RI peptide was particularly enhanced. The rank order of the velocities was similar: L2P1>L2P2>(Dummy>)KAT>control.

**Figure 8:** Oral administration of RI peptides did not alter the pattern of $A\beta_{42}$ deposits in the *Drosophila* brain. Flies treated with KAT-RI (A), L2P1-RI (B), L2P2-RI (C), TAT-KAT-RI (D), TAT-L2P1-RI (E), TAT-L2P2-RI (F), TAT-Dummy-RI (G) and water (H) all exhibited similar deposits of Aβ-reactive material (arrow, stained with 6E10 antibody).

| Name | Sequence |
|---|---|
| KAT-RI | mltakag-NH2 |
| L2P1a-RI | nstaksf-NH2 |
| L2P1b-RI | pagnstaksfsa-NH2 |
| L2P2a-RI | attakvp-NH2 |
| L2P2b-RI | pagattakvpsa-NH2 |
| Tat-KAT-RI | rrrqrrkkrmltakag-NH2 |
| Tat-L2P1-RI | rrrqrrkkrnstaksf-NH2 |
| Tat-L2P2-RI | rrrqrrkkrattakvp-NH2 |
| TAT-dummy-RI | rrrqrrkkrgggggggg-NH2 |
| iAβ5 | LPFFD-$NH_2$ |

**Table 1**: PCA derived retro-inversed sequences and related sequences with retro-inversed TAT-fusions to promote intracellular uptake for drosophila melanogaster studies.

# Figure 1

a) Inhibition

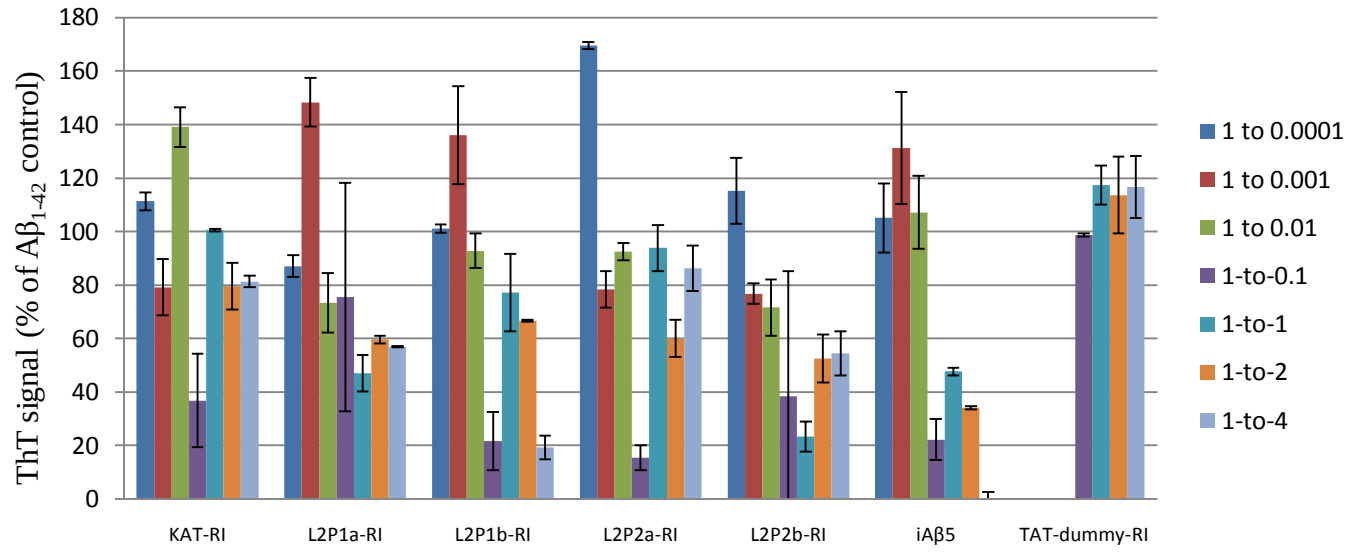


b) Reversal

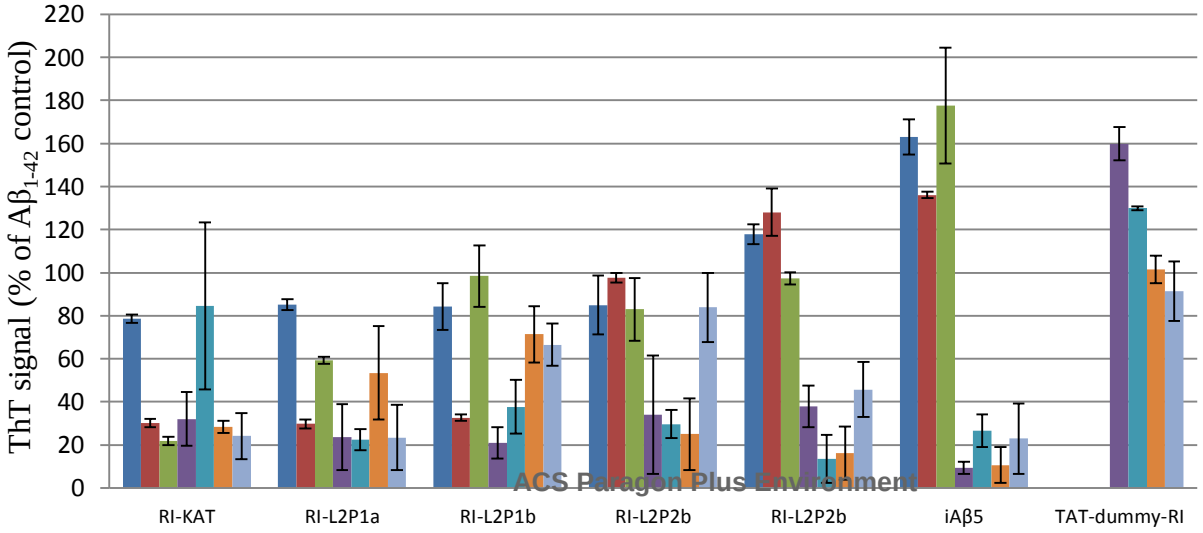

# Figure 2

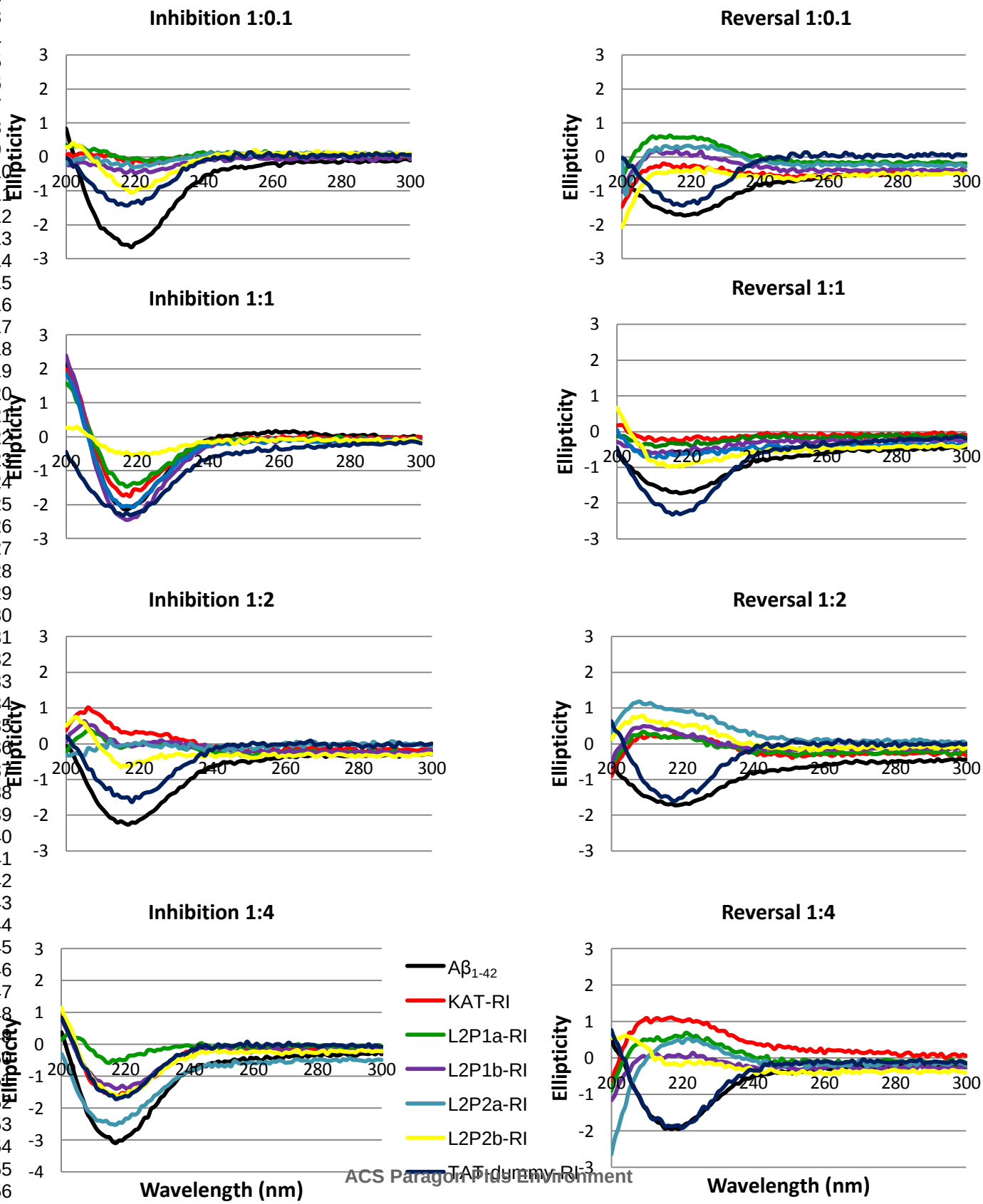

# Figure 3

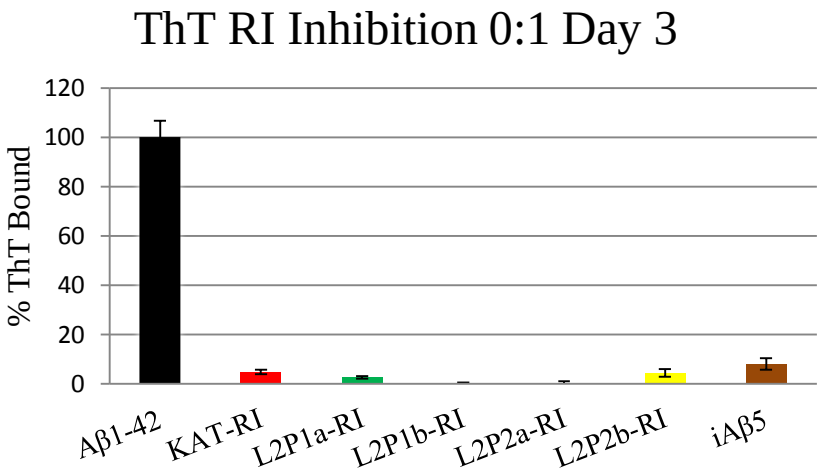
ThT RI Inhibition 0:1 Day 3
% ThT Bound
120
100
80
60
40
20
0
Aβ1-42
KAT-RI
L2P1a-RI
L2P1b-RI
L2P2a-RI
L2P2b-RI
iAβ5

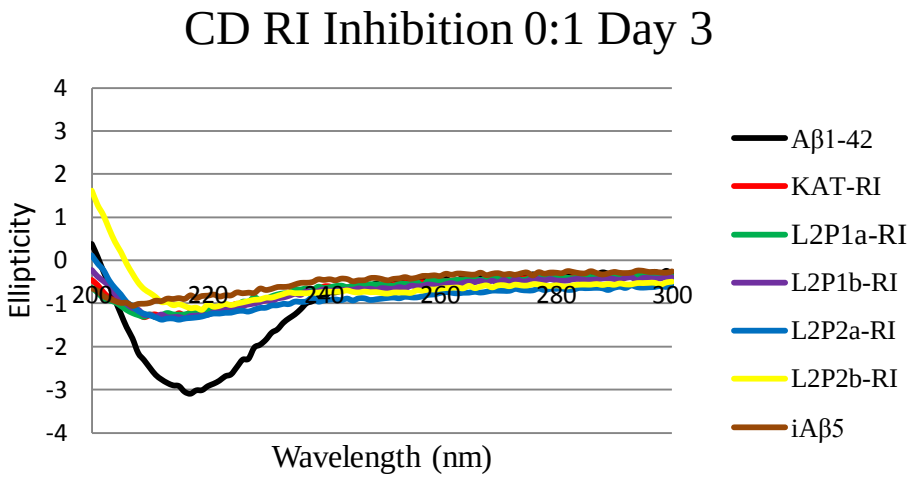
CD RI Inhibition 0:1 Day 3
Ellipticity
4
3
2
1
0
-1
-2
-3
-4
200
220
240
260
280
300
Wavelength (nm)
Aβ1-42
KAT-RI
L2P1a-RI
L2P1b-RI
L2P2a-RI
L2P2b-RI
iAβ5

# Figure 4

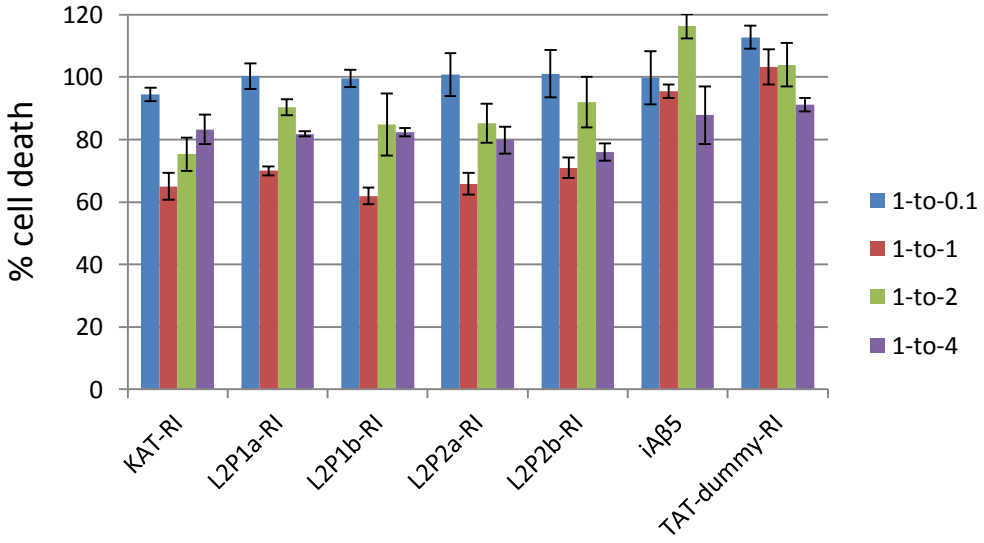
120
100
80
60
40
20
0
% cell death
KAT-RI
L2P1a-RI
L2P1b-RI
L2P2a-RI
L2P2b-RI
iAβ5
TAT-dummy-RI
1-to-0.1
1-to-1
1-to-2
1-to-4

Inhibition experiments at 1:4 Stoichiometry

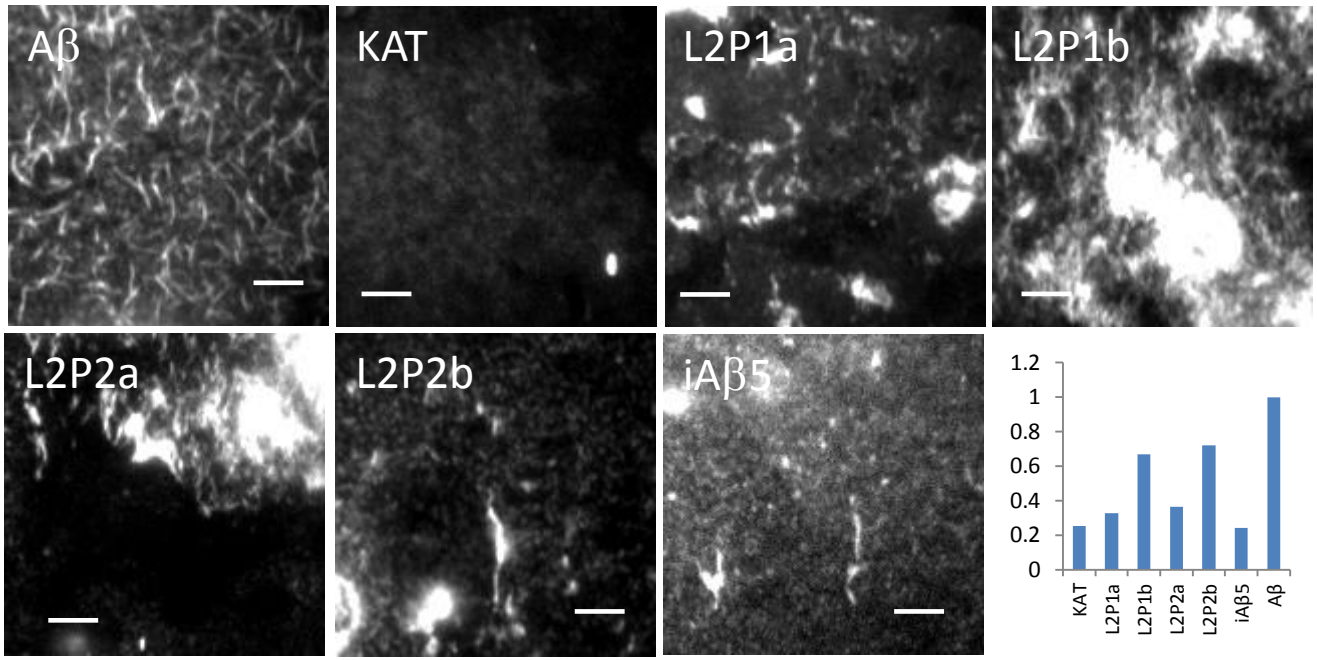

# Figure 5b

Reversal experiments at 1:4 Stoichiometry

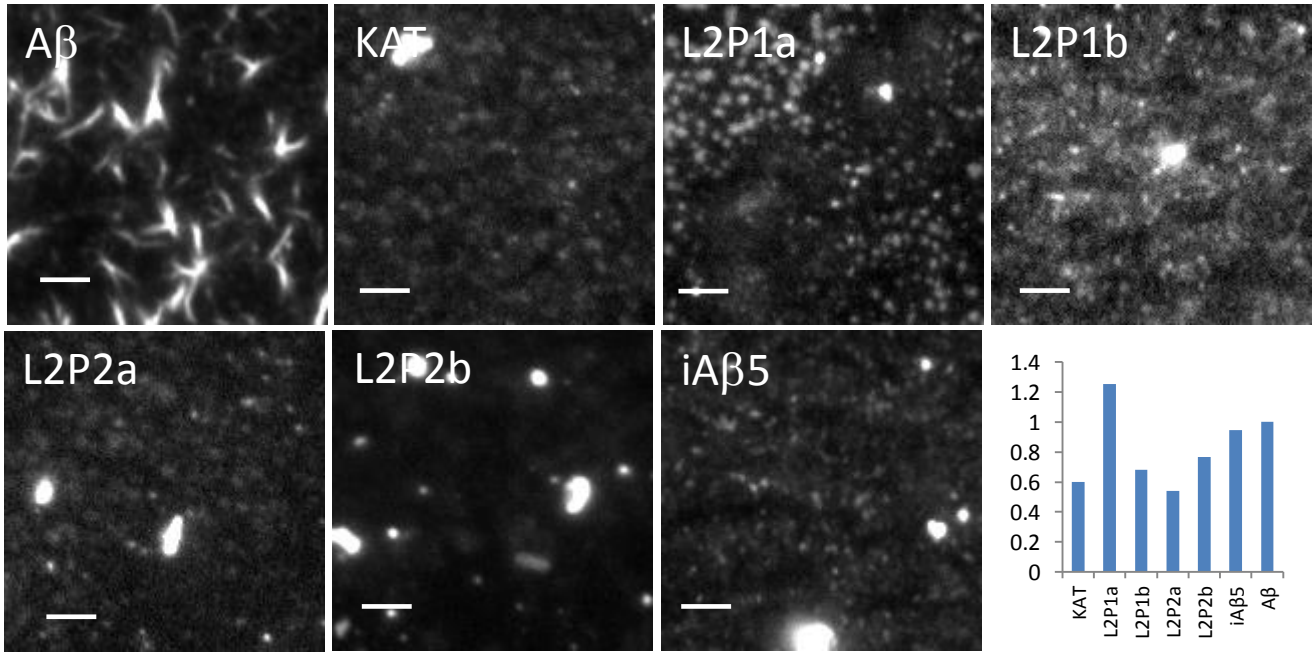

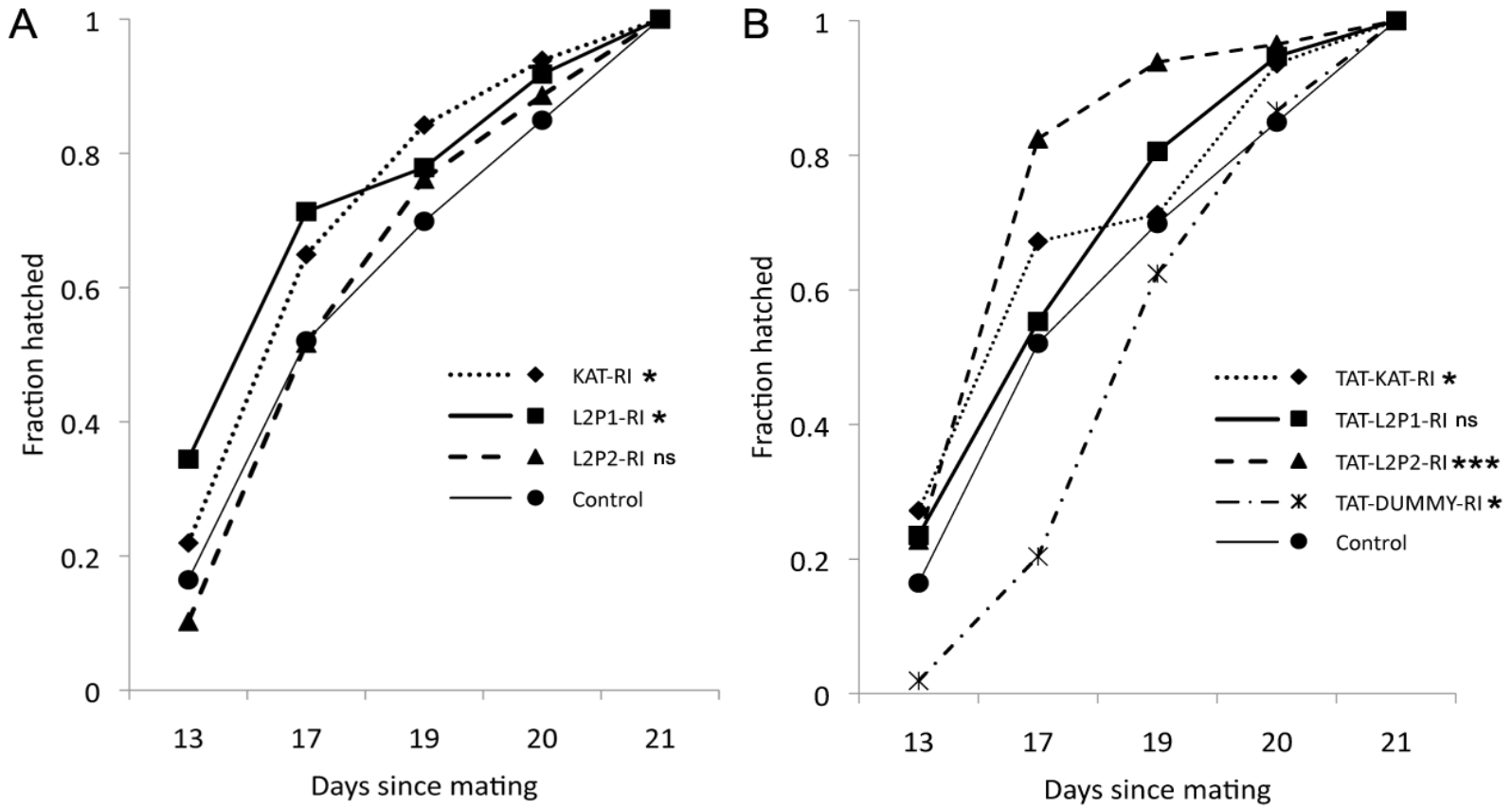
A
Fraction hatched
1
0.8
0.6
0.4
0.2
0
13
17
19
20
21
Days since mating
KAT-RI *
L2P1-RI *
L2P2-RI ns
Control
B
Fraction hatched
1
0.8
0.6
0.4
0.2
0
13
17
19
20
21
Days since mating
TAT-KAT-RI *
TAT-L2P1-RI ns
TAT-L2P2-RI ***
TAT-DUMMY-RI *
Control

# Figure 7

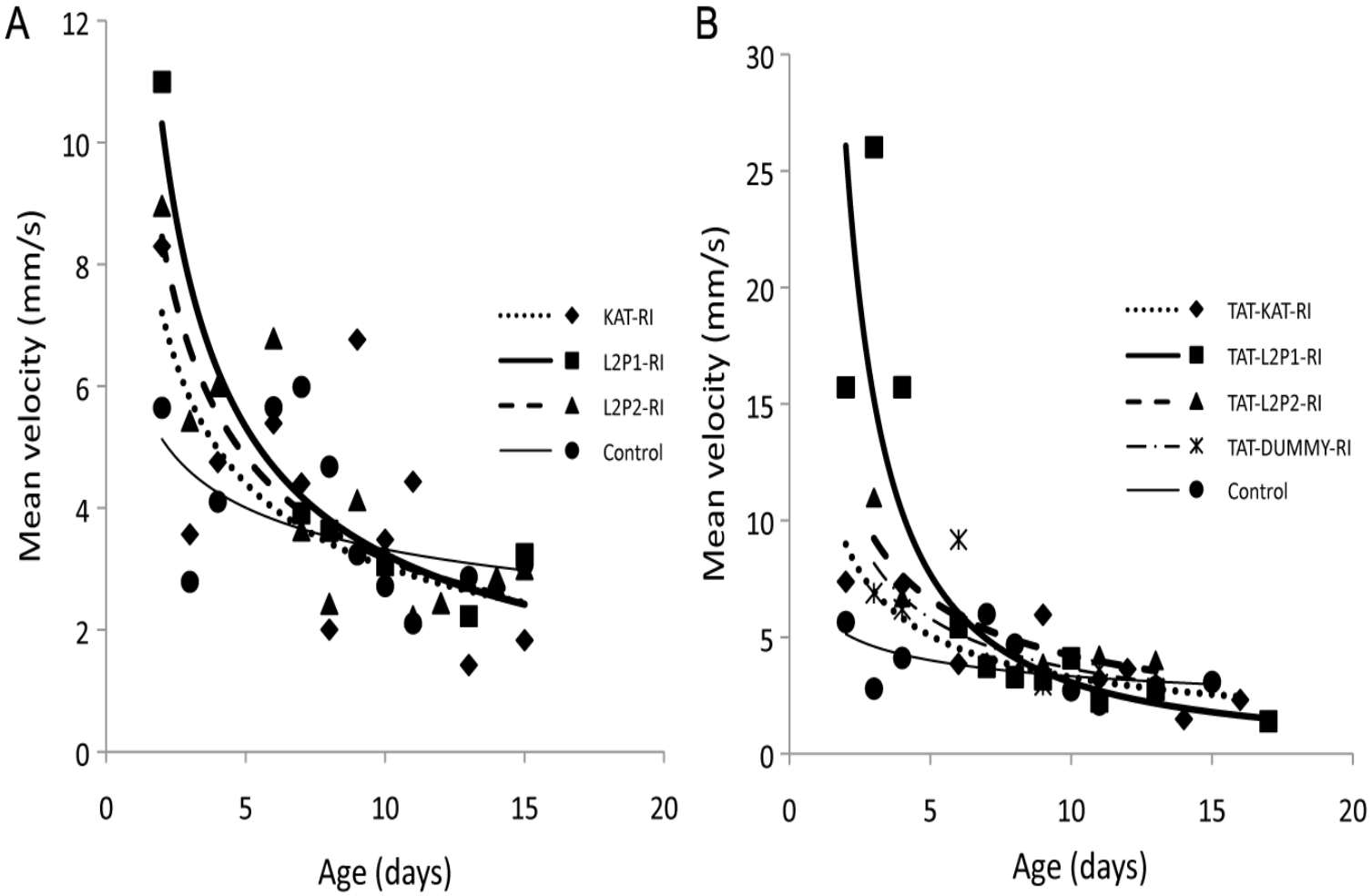
A
Mean velocity (mm/s)
Age (days)
KAT-RI
L2P1-RI
L2P2-RI
Control
B
Mean velocity (mm/s)
Age (days)
TAT-KAT-RI
TAT-L2P1-RI
TAT-L2P2-RI
TAT-DUMMY-RI
Control

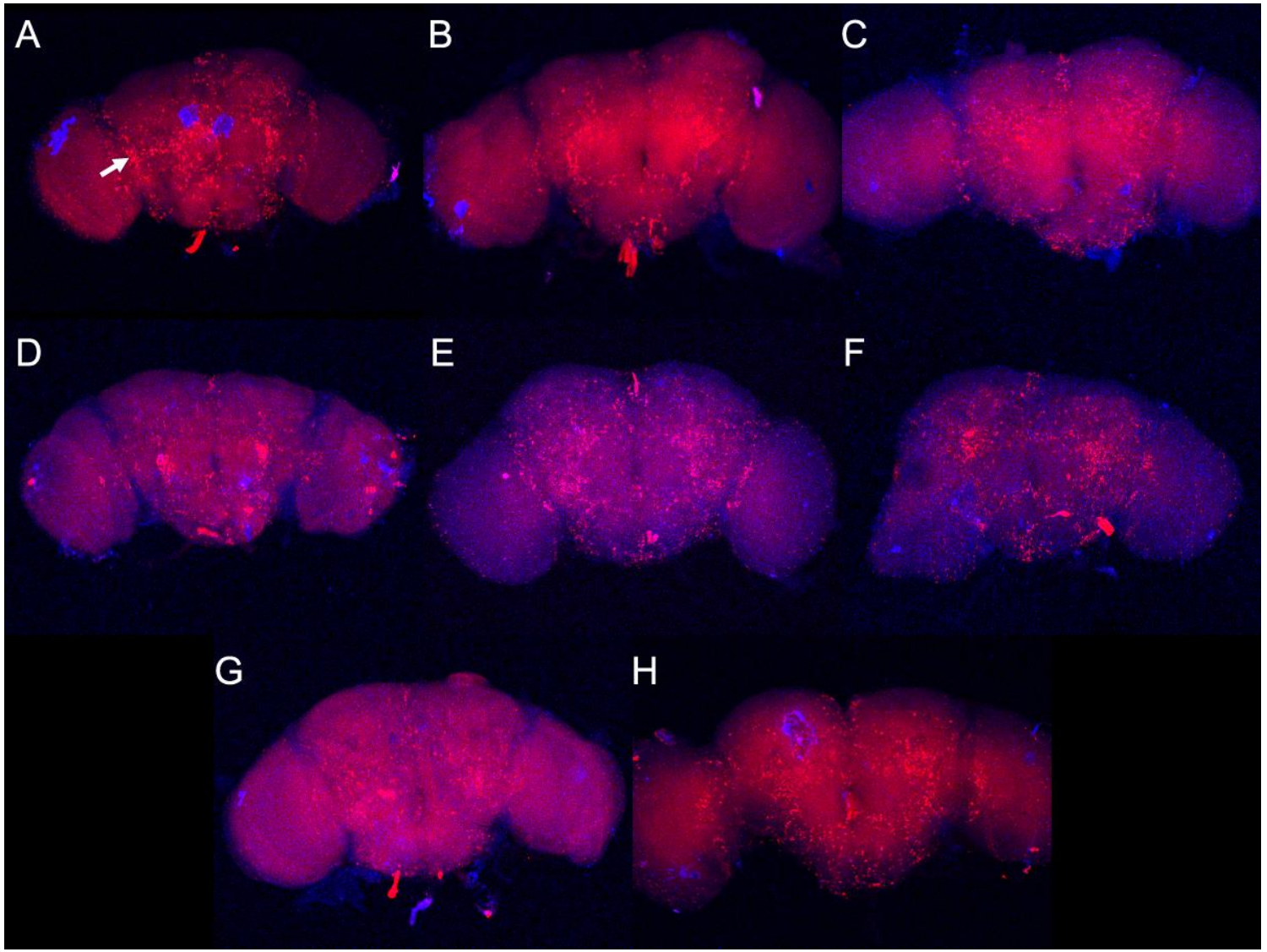
A
B
C
D
E
F
G
H